

## A New MOSFET IC Laser-Driver With On-Chip Thermal and Optical Stabilization

F. Almarzouki, Adel El-Hennawy, Said Al-Ghamdi  
and S.S. Al-Ameer

Faculty of Science, Physics Department, King Abdulaziz University,  
P.O. Box 9028, Jeddah 21413, Saudi Arabia

**ABSTRACT.** This paper presents a new more advantageous configuration for the laser diode that is used as the principle light source in optical fiber communications and a range of other applications. Most of the common drawbacks have been eradicated through the new design which is integrated through the well known floating gate MOSFET technology. Advantages including improved thermal and optical stabilization and easy direct modulation are realized from a new on-chip laser driver. Besides, the technique guarantees compensation for device leakage and device to device tolerances. The resulting device is cheaper and easy to construct.

The voltage control provides better output power modulation and improve linearity for high output power levels. The threshold current required to stimulate emission is also reduced to  $\sim 10^3$  A/cm<sup>2</sup> at 300 K with an active region thickness of  $\sim 0.5$   $\mu$ m. In fact the proposed design provides a thinner well defined active region (0.3  $\mu$ m) which also acts as an optical cavity resonator, besides satisfying the conditions for the confinement of charged carriers and optical fields.

Great efforts have been made, in the early 1970's, in research in optical communications and related areas. This resulted in significant technological advances in optical sources and led in turn to the birth of the semiconductor laser diode which is, now, the principal light source used for optical fiber communications. This device has adequate output power for a wide range of applications; its optical output can be directly modulated. It has a high efficiency and

its dimensional characteristics are compatible with the optical fiber. The major aspects of lasers, their constructions, and principles of operation are available in literature (Wilson and Hawkes 1983, Verdeyen 1981, Kressel and Butler 1977, El-Hennawy and Al-Ghamdi 1993, El-Hennawy *et al.* 1993).

The optical energy released from these devices has spatial and temporal coherence which means it is highly monochromatic ( $\lambda \sim 0.1$  to  $1 \text{ \AA}$ ) and the output beam is very directional ( $\theta_{\parallel} \sim 5^\circ$  and  $\theta_{\perp} \sim 30^\circ$ ) (Verdeyen 1981, Kressel and Butler 1977, El-Hennawy *et al.* 1993). However, laser diodes are not easy to use without employment of complex drive circuitries and thermal and optical stabilization schemes (El-Hennawy and Al-Ghamdi 1992) which are expensive to realize and have relatively low yield (Kressel and Butler 1977, El-Hennawy *et al.* 1993).

In this paper we present a new MOSFET IC original configuration, to be integrated on the same chip with the laser source, to control and smooth up the output power level and stabilize the system against temperature variation and aging. It also provides direct-modulation facility.

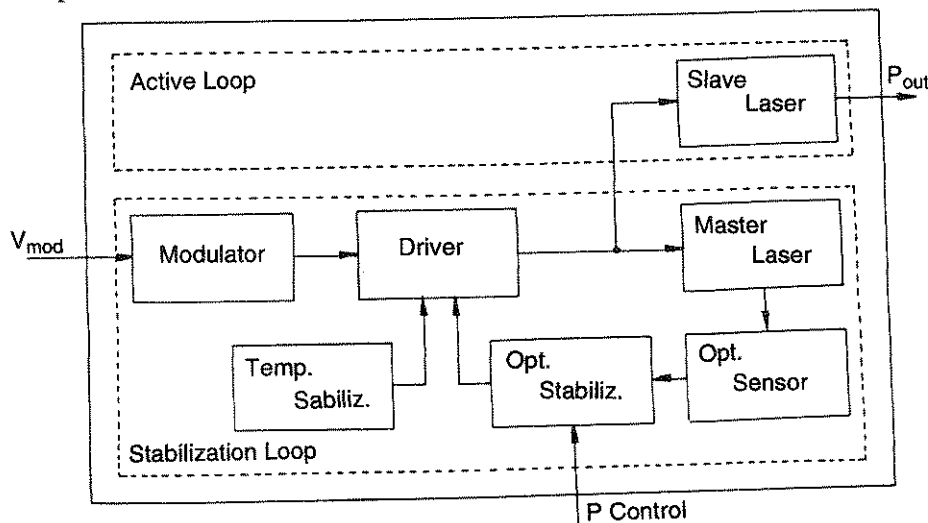


Fig. 1. Block diagram of proposed laser configuration.

### 1. Laser Source

Figure (1) shows the block diagram of the proposed laser configuration with on-chip thermal and optical stabilization, output-power level control and modulation. It is constructed of two basic loops; one is the active loop which contains the master laser and the thermal and optical stabilization circuitries. This loop is responsible for

giving two voltage signals, one is proportional to the output power level and the second is proportional to the operating temperature. These signals are fed through a negative feedback loop to the laser driver so as to smooth up the output power level and to compensate for the effects of the operating temperature variations and the device aging. Supplementary circuitries are introduced for controlling the output power level and allowing for modulation.

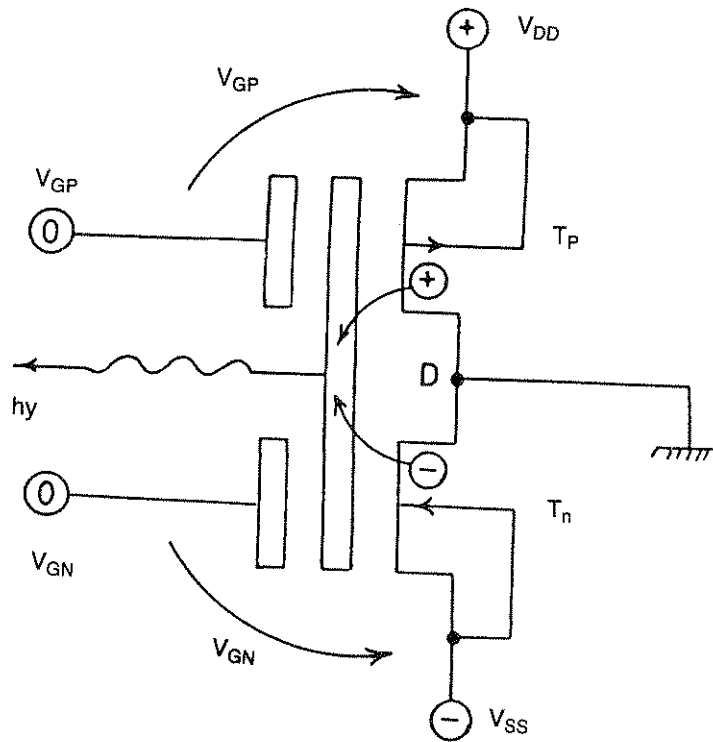


Fig. 2. MOSFET laser source structure.

### 1.1 Laser MOSFET

It is constructed, as shown in Fig. (2), with a floating gate CMOS inverted  $T_p$  and  $T_n$  whose floating gate is common for the two MOSFET's. A non doped GaAs compound (Wilson and Hawkes 1983, Verdeyen 1981, Kressel and Butler 1977, El-Hennawy and Al-Ghamdi 1992, El-Hennawy *et al.* 1993), is used, to realize the floating gate. The common drain D is catted while the sources of  $T_p$  and  $T_n$  are biased to  $V_{DD}$  and  $V_{SS}$  respectively ( $V_{DD} = V_{SS} = 10$  V). The gates of  $T_p$  and  $T_n$  are biased respectively to  $V_{GP}$  and  $V_{GN}$  which should be equal ( $V_{GP} = V_{GN} = 0$ ) in

absence of feedback (stabilization loop is disconnected). The channel length  $L$ , width  $Z$ , first oxide thickness (between the channel and floating gate)  $h_0$  and second oxide thickness (between the floating and control gates)  $h_1$  are  $1 \mu\text{m}$ ,  $400 \mu\text{m}$ ,  $400 \text{ \AA}$  and  $800 \text{ \AA}$ , respectively. To keep the floating gate potential  $V_{FG}$  as great as possible (greater value of  $V_{FG} = V_{GP} = V_{GN}$ ) the technique shown in Fig. 3 is used. In this

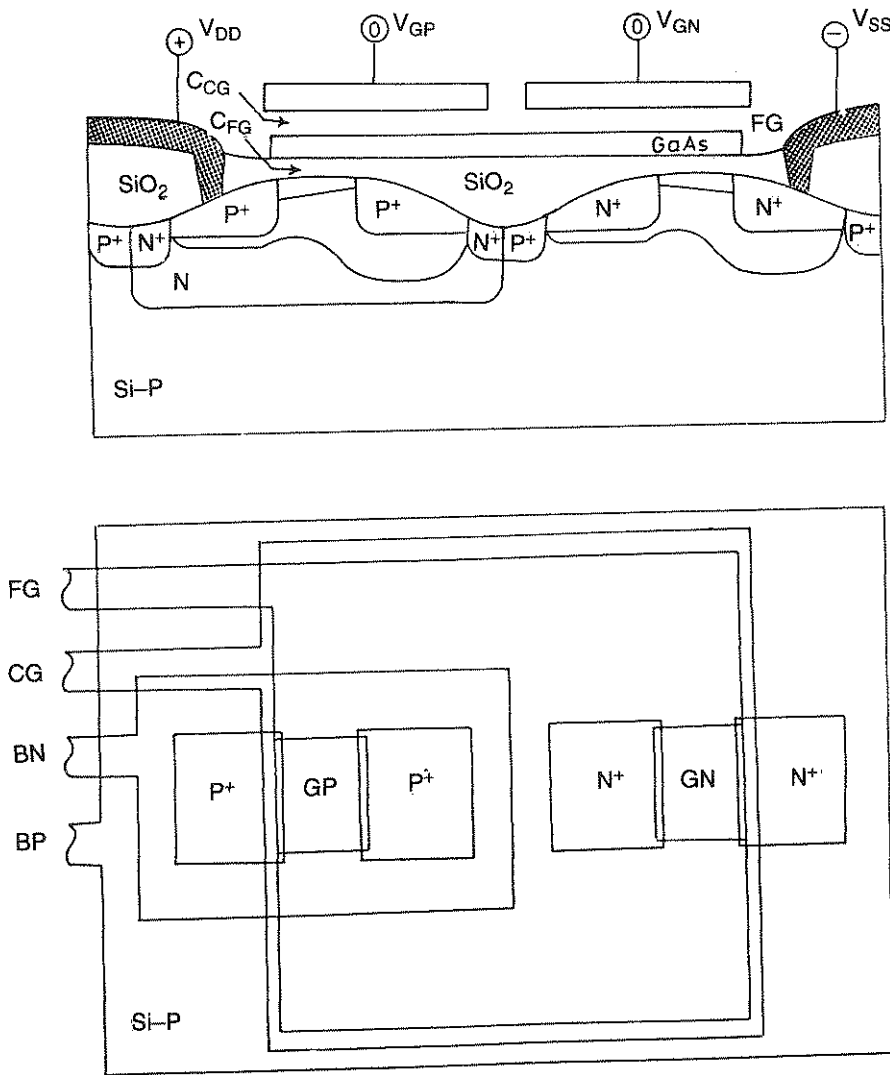


Fig. 3. Configuration to maximize floating gate potential.

case the overlapping area between the control and the floating gates is kept much greater than that between the floating gate and the channel. Hence the floating gate to control gate capacitance  $C_{CG}$  will be much greater than that existing between the floating gate and the channel  $C_{FG}$  (El-Hennawy 1992, El-Hennawy and Al-Ghamdi 1992).

The operation of the laser MOSFET is as follows; the drain-source voltages of  $T_p$  and  $T_n$  are sufficient to heat up the channel carriers and enables them to jump over the Si-SiO<sub>2</sub> interface barrier (El-Hennawy and Al-Ghamdi 1992, El-Hennawy and Mobarek 1993). Since the control gate of  $T_p$  is negative with respect to its source and that of  $T_n$  is positive with respect to its source, then hot holes and hot electrons are simultaneously injected into the floating gate. The design values of  $L$  and  $Z$  of  $T_p$  and  $T_n$  are modified so as to make the hot-hole current  $I_{gp}$  exactly equal to the hot-electron current  $I_{gn}$ . In this case the net floating-gate current  $I_g = I_{gp} - I_{gn}$  is zero, regardless of the level of carrier pumping or power output, which means null floating-gate power dissipation. This will guarantee greater output power levels and better linearity. Also no charge builds up in the floating gate which keeps its potential  $V_{FG} = 0$  and consequently sustains high carrier acceleration into it all the time. Also smaller losses and higher efficiency are expected due to better homogeneity of the floating gate material and no gate heating takes place because it is not doped (Wilson and Hawkes 1983, Verdeyen 1981, El-Hennawy *et al.* 1993).

The electrons and holes pumped into the GaAs floating gate recombine radiatively and release radiation energy  $h\nu$  with  $\nu$  being the radiation frequency determined by the energy gap  $E_g$  ( $h\nu = E_g$ ). The floating gate is surrounded by highly clean SiO<sub>2</sub>. It has a refractive index ( $n_{or} = 1.4$ ) which is smaller than that of GaAs ( $n_a = 3.6$ ) and an energy gap  $E_g = 8.1$  eV which is greater than that of GaAs (1.43 eV) and thus it provides the desired dual confinement for charge carriers and optical fields and acts at the same time as an optical resonant cavity. Since the quantum transitions here occur between nearly discrete energy levels, then the radiation of the new device will have spatial and temporal coherence and will be highly monochromatic and highly directional ( $\theta_{||} \sim 5^\circ$   $\theta_{\perp} = 30^\circ$ ) and  $\lambda \sim 0.1 - 1 \text{ \AA}$ ). In addition, the floating gate thickness is very small ( $\sim 0.3 \text{ \mu m}$  or less) which increases the fraction of radiative recombination and decreases the absorption of the emitted radiation by the active region it-self (Wilson and Hawkes 1983, El-Hennawy *et al.* 1993).

The output power is given by (Wilson and Hawkes 1983):

$$P_o = ZL (J_g - J_{gth}) \eta_i \frac{hv}{q} \frac{\left( \frac{1}{2Z} \ln \frac{1}{R_1 R_2} \right)}{\left( \gamma + \frac{1}{2Z} \ln \frac{1}{R_1 R_2} \right)}; J_g > J_{gth}$$

$$J_{th} + \frac{8\pi v_0^2 q t v n^2}{\eta_i C^2} \left( \gamma + \frac{1}{2Z} \ln \frac{1}{R_1 R_2} \right)$$

With:  $q$  the electron charge ( $1.6 \times 10^{-19}$  C)

$t$  the floating gate thickness  $\sim 0.3 \mu\text{m}$

$\eta_i$  internal efficiency

$Z$  the floating-gate width

$R_1, R_2$  the reflectivities of the floating gate internal surfaces.

$v$  line width

$\gamma$  loss efficiency

### 1.2 Design Considerations

The MOSFET channel length  $L = 1 \mu\text{m}$  or less is experimentally suitable for offering the carrier heating required to give a hot carrier gate current density which is greater than the threshold value ( $\sim 562 \text{ A/m}^2$ ) needed for lasing (El-Hennawy and Al-Ghamdi 1992, El-Hennawy and Mobarek 1993). The channel width  $Z$  (which represents the active region length) is taken  $400 \mu\text{m}$  which is much greater than both the active region width ( $10 \mu\text{m}$ ) and thickness ( $0.3 \mu\text{m}$ ) to guarantee a limited number of modes (El-Hennawy 1992, Shahab and El-Hennawy 1990) and therefore, results, in smaller losses and modal noise, and gives better coherence and directionality and improves the device reliability (Wilson and Hawkes 1983, El-Hennawy *et al.* 1993). The HMOS II technology design rules are used.

## 2. Laser Driver

It consists, as shown in Fig. 4, of a differential input stage  $T_2, T'_2$  which is biased and loaded with current sources  $T_2, T'_2$ . A common mode feedback technique

is inserted using  $T_3$ ,  $T_4$  and  $T_5$  to stabilize all node voltages and branch currents against ambient temperature variations and circuit aging (El-Hennawy and Shahab 1990). The difference amplifier is designed so as to give  $V = 0 = V'_0$  in the absence of feedback and modulating signals. It has a difference mode gain of 200, and input offset voltage of about 2 mV and voltage drift of  $20 \mu\text{V}/^\circ\text{C}$ . These characteristics are sufficient for our applications.

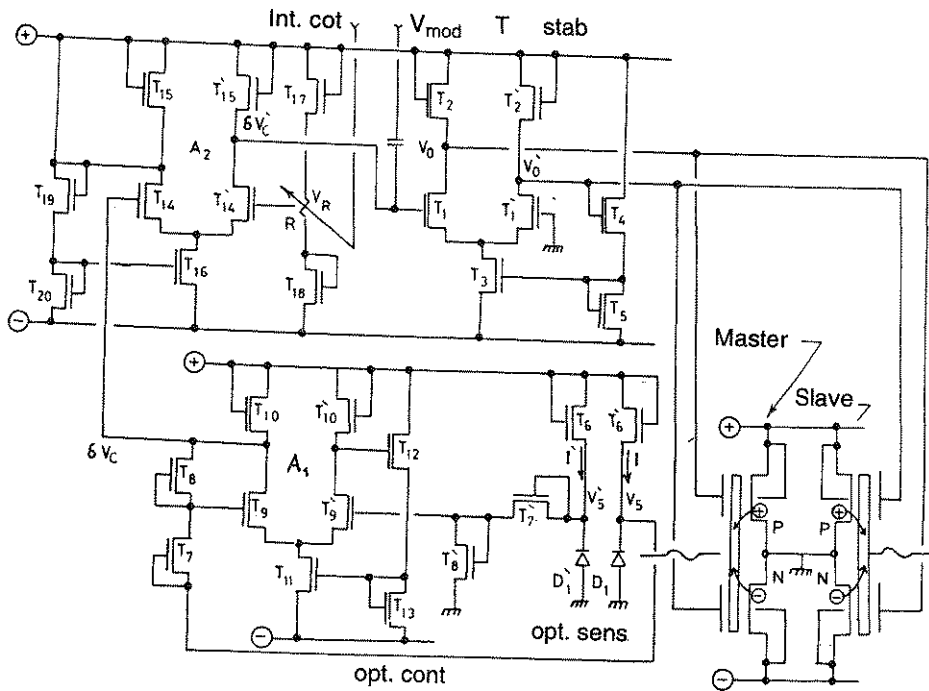


Fig. 4. Laser driver circuit configuration.

### 2.1 Radiation Level Monitoring

It is composed of two branches, the first ( $T_6$ ,  $D_1$ ) is responsible of sensing the radiation and gives a voltage signal which is proportional to it together with the diode leakage. The second ( $T'_6$ ,  $D'_1$ ) is shielded from radiation then it gives a voltage signal which is proportional to the leakage current  $I_L$  of diode  $D'_1$ . The second signal is used to compensate for the leakage of the diode  $D_1$  and therefore to have a signal which is purely proportional to the radiation level (El-Hennawy and Al-Ghamdi 1992, El-Hennawy and Shahab 1990). A difference amplifier ( $T'_9$ ,  $T'_{10}$ ,  $T_9$ ,  $T_{10}$  and  $T_{11}$ ) is implemented to carry out this compensation. This signal is compared, by the

difference amplifier ( $T_{14}$ ,  $T_{15}$ ,  $T'_{14}$ ,  $T'_{15}$  and  $T_{16}$ ) to a reference voltage  $V_R$  which is responsible of determining the laser output – power level. The MOSFET string  $T_{17}$ ,  $T_{18}$  and the variable resistance  $R$  are designed so as to allow variation of the output power level between two prescribed upper and lower limits. Supplementary MOSFET configurations similar to that used to stabilize the driver are employed here for the same purpose.

### 2.2 Theory of Operation

When the current  $I$  of the diode  $D_1$  increases by  $\delta I \ll I$  due to exposure to radiation from the master laser, the source voltage  $V_s$  of the MOSFET  $T_6$  decreases by  $\delta V_s$  so as to accommodate this current variation. Straightforward analysis showed that the corresponding control signal  $\delta V_c = \delta V_s - \delta V'_s$  (after amplification and leakage compensation) is given by:

$$\delta V_c = \frac{G_1 k}{1} \delta I$$

where  $G_1$  is the voltage amplification of the amplifier  $A_1$ .

If the intensity of radiation (determined by the value of  $V_R$ ) is so that  $\delta V_c = V_R$ , the output  $\delta V'_c$  from the amplifier  $A_2$  is zero and  $V_0$  and  $\delta V'_0$  of the driver remain unchanged ( $V_0 = \delta V'_0 = 0$ ). If  $\delta V_c$  increases (due to an increase of radiation intensity and becomes greater than  $V_R$ ), then  $\delta V'_c$  increases and causes  $V_0$  to decrease and  $V'_0$  to increase. In this case  $V_{GSN}$  of  $T_n$  and  $V_{GSP}$  of  $T_p$  are decreased which shifts down the carrier pumping into the floating gate and tends to decrease the radiation intensity and the value of the control signal  $\delta V_c$ . This process continues to decrease  $\delta V_c$  till it becomes equal to  $V_R$ . The contrary occurs in the case when the radiation intensity decreases. If  $V_R$  is increased (or decreased),  $\delta V'_c$  decreases (or increases) and  $V_0$  increases (or decreases) while  $V'_0$  decreases (or increases). Therefore this tends to increase (or decrease)  $V_{GSN}$  of  $T_n$  and  $V_{GSP}$  of  $T_p$  which shifts up (or shifts down) the carrier pumping into the floating gate and causes the radiation intensity to increase (or to decrease).

### 2.3 Laser Beam Modulation

The beam modulation is achieved by the  $V_{mod}$  voltage which is externally introduced and superimposed on the power-level monitoring signal  $\delta V'$  coming from the output of the amplifier  $T_{14}$ ,  $T_{15}$ ,  $T'_{14}$ ,  $T'_{15}$  and  $T_{16}$  and fed into the amplifier  $T_1$ ,  $T_2$ ,  $T'_1$ ,  $T'_2$  and  $T_3$ . The two outputs  $V_0$  and  $V'_0$  of this amplifier which are



complementarily varying are used to control the carrier pumping (electrons and holes) from the channels of MOSFET's  $T_n$  and  $T_p$  into the floating gate. When  $V_{mod}$  increases (decreases),  $V_0$  decreases (increases) and  $V'_0$  increases (decreases) proportionally. This leads to reduce (increase) gate to source voltages of MOSFET's  $T_n$  and  $T_p$ , therefore, results in a smaller (greater) carrier pumping level and smaller (greater) radiation-power level.

### Results and Discussions

This section presents the experimental results that characterise both the MOSFET laser and its on-chip driver. Comparison with the theory is also provided where appropriate along with a general discussion of the findings.

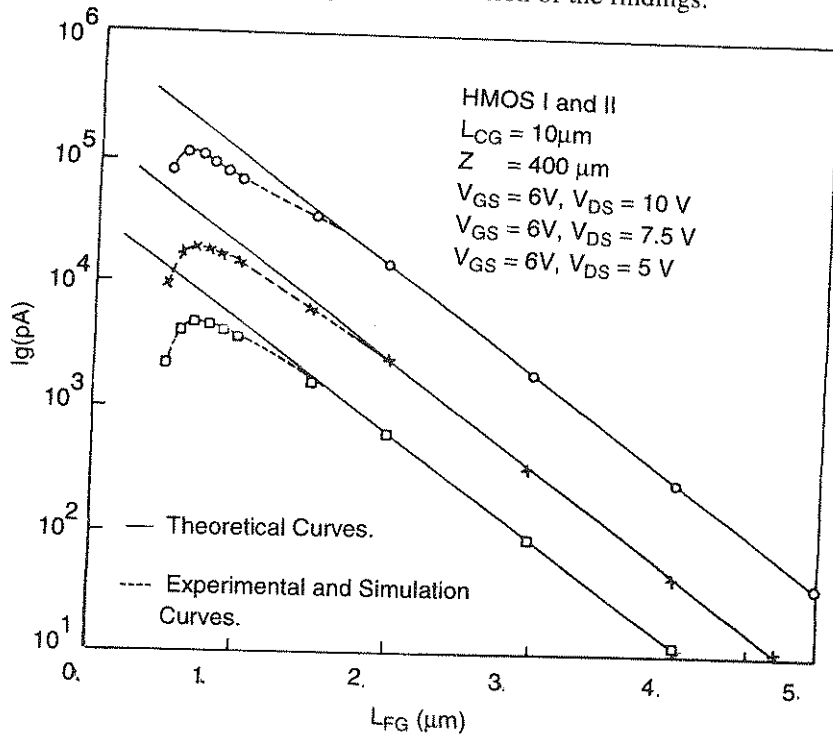


Fig. 5. Variation of  $I_g$  at three different values of  $V_{DS}$ .

#### MOSFET Laser Characterization

Figure (5) shows the variation of  $I_g$  (which is responsible for the carrier-pumping level) with the MOSFET biasing voltages  $V_{GS}$  and  $V_{DS}$  (~ 6 to 10 V)

for different values of device geometry (channel length  $L \sim 5$  to  $0.5 \mu\text{m}$  and channel width  $Z = 400 \mu\text{m}$ ). It can be observed that  $I_g$  increases as  $L$  is reduced and/or  $V_{DS}$  increased. Values of resulting current density  $J_g$  as high as  $10^3 \text{ A/m}^2$  can be achieved, which are larger than the magnitude of the threshold current required to excite the device lasing ( $J_{th} \sim 300$  to  $500 \text{ A/m}^2$ ). A comparison of these experimental findings with the theoretical predictions shows an excellent match from channel lengths greater than  $1.5 \mu\text{m}$ .

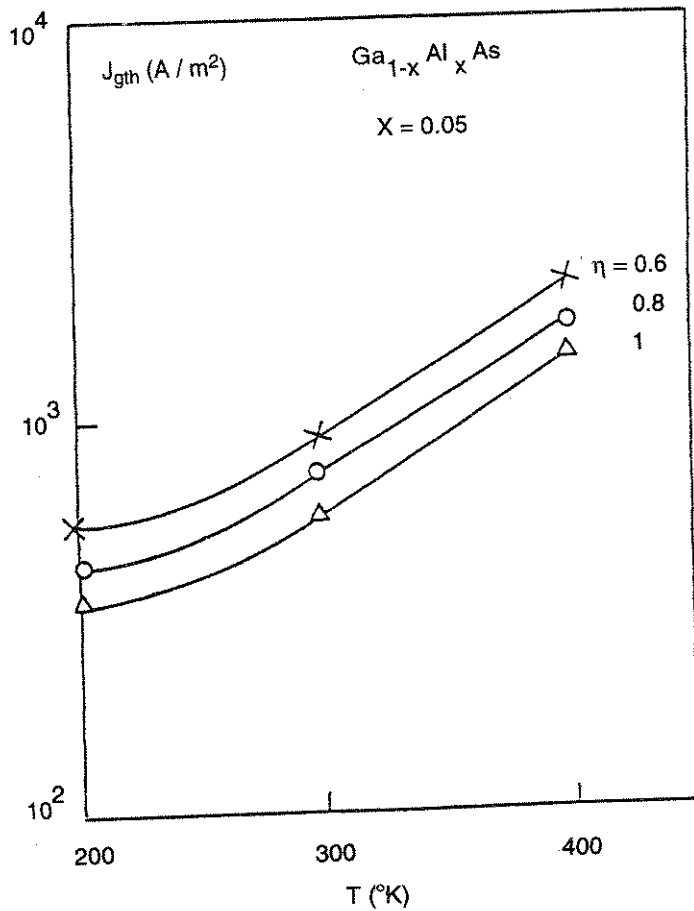


Fig. 6. Variation of  $J_{gth}$  with temperature at three different values of quantum efficiency  $\eta$ .

In Figure (6) the variation of threshold current density  $J_{gth}$  is depicted against temperature  $T$  at different values of quantum efficiency  $\eta_i$ . It is found that  $J_{gth}$  increases with increasing  $T$ , while a higher value of quantum efficiency results in low threshold current density. It can be inferred from these findings that it is

preferable to operate the laser source at low temperature in order to keep the active region as cold as possible. As a consequence, power losses caused by crystal and defects scattering would be reduced. These possible improvements were actually observed during the course of this study.

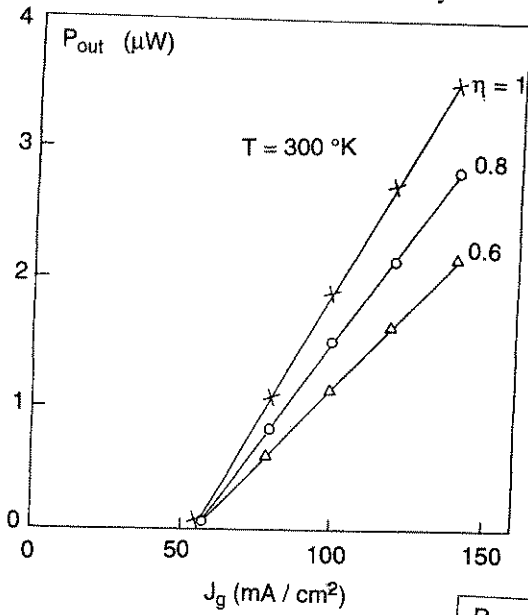


Fig. 7a. Variation of  $P_{out}$  with  $J_g$  at different values of quantum efficiency  $\eta$ .

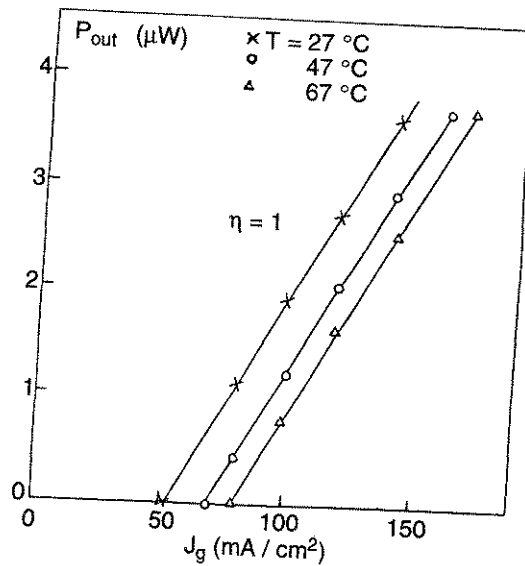


Fig. 7b. Variation of  $P_{out}$  with  $J_g$  at different values of temperature.

Figures (7a, b) show the variation of  $P_{out}$  with the pumping current density  $J_g$  for different values of  $\eta_i$  and  $T$ .  $P_{out}$  increases by increasing  $J_g$  and /or decreasing  $T$ .

This is because the number of radiative recombination increases with  $J_g$ . The output radiations also intensify at high quantum efficiency because the latter translate into low active zone losses. Conversely, the losses increase at high temperatures which are generated either internally through high intensity fields or externally by heating. As a result the efficiency and output power drop.

In the present design, the dual carrier, whereby electrons and holes are simultaneously injected through the oxide layer into the floating gate, results in null current and therefore no power is dissipated in the active zone. This keeps the active zone temperature low and smooth and provides the linearity in the response.

#### Driver Characterization

Figure (8) shows the variation of driver voltage  $V_0$  and  $V'_0$  with the radiation intensity (indicated as variations in  $\delta V_c$ ). Nonlinearity is observed at high radiation intensity. It is associated with amplifier's saturation, and also as the detector becomes no longer linear.

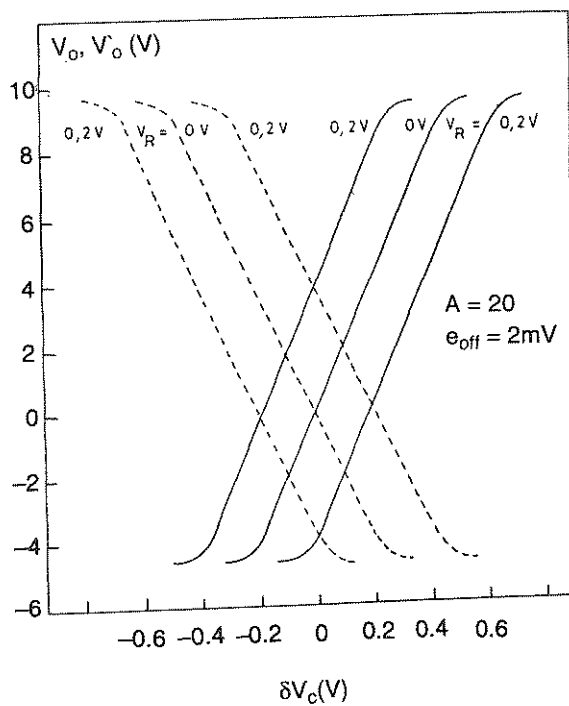


Fig. 8. Variation of  $V_0$ ,  $V'_0$  with radiation intensity  $\delta V_c$ .

Figures (9) and (10) shows the variations of the driver voltage  $V_0$  and  $V'_0$  and the radiation power intensity  $P_{out}$  (expressed by  $\delta V_C \cdot I_{pA}$ ) with temperature. Insertion of the feedback loop appreciably decreases the dependence of the radiation and the voltages  $V_0$  and  $V'_0$  on the variations of the ambient temperature  $T$ .

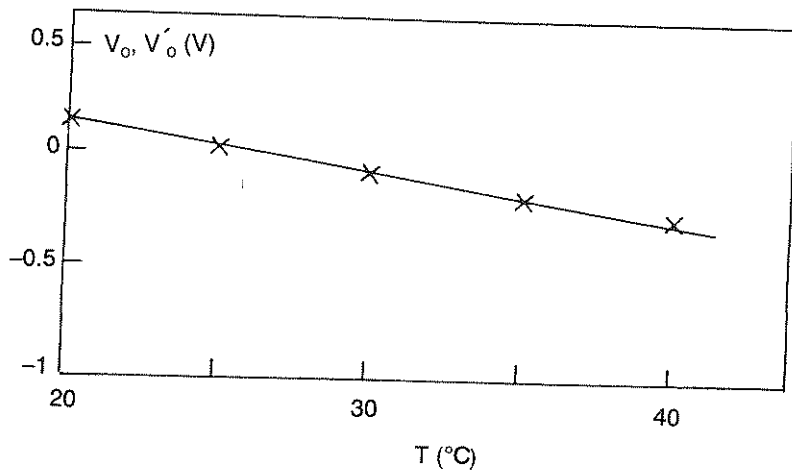


Fig. 9. Variation of  $V_0, V'_0$  with temperature.

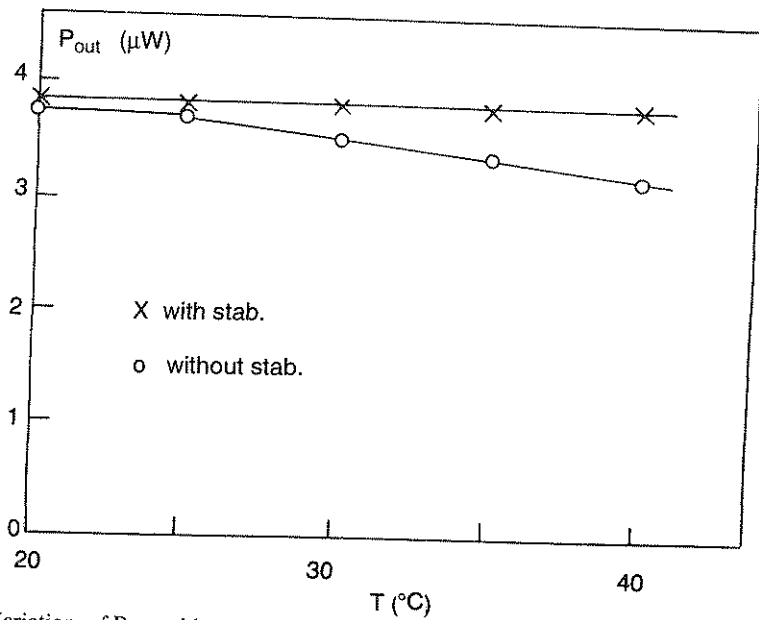


Fig. 10. Variation of  $P_{out}$ , with temperature.

### Conclusions

A new MOSFET integrated laser source is devised and characterised through intensive experimentation. It has been found to function well under different operating conditions and excellent agreement between the findings and analytical models are achieved. Some of the main advantages include very high power levels at linearity better than 2% and near zero temperature sensitivity.

### References

- El-Hennawy, A., Al-Mrzouki, F. and Al-Ghamdi, S.** (1993) Study and Characterization of a New Floating Gate MOSFET Laser Source, 18th Int. conf. for SCSSDR Cairo, Egypt, 349-351 pp.
- El-Hennawy, A.** (1992) Design and Simulation of Non Volatile CMOS EEPROM, *Int. J. Elect.* **72**: 37-87.
- El-Hennawy, A. and Al-Ghamdi, S.** (1992) Study and Characterization of MOSFET IC Magnets Detector, *IIE Proc.* **139**: 119-125.
- El-Hennawy, A. and Al-Ghamdi, S.** (1993) Performance Improvement of Lasers by using Trapezoidal - Gate MOSFET's, *IEEE. Proc.* **4**: 69-72.
- El-Hennawy, A. and Mobarek, O.** (1993) Precise Modling of Hot carrier Gate - Current in short - Channel MOSFET's, *IEEE Tran. Elec.* **40**: 19-45.
- El-Hennawy, A. and Shahab, W.** (1990) New Leakage Compensation Technique for Superior CFC, *Int. J. Elec.* **69**: 793-803.
- Kressel, H. and Butler, J.K.** (1977) *Semiconductor Lasers and Hetrojunction LEDS*, Academic Press, Inc., Chapter 12.
- Shahab, W. and El-Hennawy, A.** (1990) New Technique for Offset Compensation and Noise Reduction in MOSFET VLSI, *Int. J. Elec.* **68**: 547-566.
- Verdeyen, J.T.** (1981) *Laser Electronics*, Prentice Hall Int., Chapter 11.
- Wilson, J. and Hawkes, J.** (1983) *Optoelectronic: An Introduction*, Prentice Hall Int., 215-216 pp.

(Received 11/03/1997;  
in revised form 29/03/1998)

## نبائط جديدة من الـ MOSFET معمولة كمصدر ليزر وغير متأثرة بالحرارة والضوء

فهد المرزوقي و عادل الحناوي و سعيد الغامدي و سعيد الأمير

قسم الفيزياء - كلية العلوم - جامعة الملك عبد العزيز  
ص ب (٩٠٢٨) جدة ١١٤١٣ - المملكة العربية السعودية

لقد بذلت جهود عظيمة من بداية التسعينات ولا زالت لدراسة أنواع المصادر المستخدمة في الإتصالات بواسطة الالياف البصرية - ونتيجة لهذه الجهود والعمل المتواصل ظهرت نتائج ايجابية ومفيدة سواء في الأبحاث أو التقنيات لهذه المواد .

ومن نتائج هذه الأبحاث الوصول إلى ما يسمى الآن بمصادر الليزر المصنعة من اشباه الموصلات والذي اصبح مصدراً أساسياً لاغنى عنه في الاستخدامات التطبيقية المتنوعة سواء كان ذلك في الاتصالات أو المجالات الأخرى المتعددة .

لقد أثبت هذا النوع من المصادر قدرته على التحكم في كمية الطاقة المستخدمة والمنبعثة منه وتعتمد في تصنيعها على التقنية الحديثة المتقدمة جداً مما أكسبها القدرة على أن تصنع بالأبعاد والأحجام المطلوبة ومثلاً على تلك الأبعاد والتي تتراوح ابعادها ما بين  $(\Delta\lambda \sim 0.1 \text{ to } 1 \text{ \AA})$  وكذلك مصنعه باتجاهات ومقاطع هندسية  $(\theta_{\perp} \sim 30^{\circ} \text{ and } \theta_{\parallel} \sim 5^{\circ})$  .

ومما لاشك فيه انه ليس من السهولة التحكم في هذه الأبعاد ولكن للتغلب



على هذه الصعوبات فقد عملت مكونات من الدوائر الكهربائية المساعدة والتي تتم بها عملية التحكم في عمل هذه المصادر وسوف يتطرق هذا البحث إلى هذه الدوائر المساعدة والتي أثبتت مقدرتها الفائقة على التغلب على هذه العقبات وخاصة التغير الحراري والضوئي والذي يسبب مشاكل كبيرة لمثل هذه المصادر عادة .

وكما هو معروف أهمية المصادر الكهروضوئية في التقدم التقني . وتعتبر الثنائيات الليزرية من أساسيات الخلايا الكهروضوئية المستخدمة في الاتصالات وكذلك في مجالات تطبيقية أخرى متعددة .

ويختص هذا البحث بدراسة شكل جديد من اشكال الليزر يمتاز بأفضليته عن الموجود حالياً لأنه خالي من العوائق التصنيعية والتقنية حيث أن هذا المصدر الكهروضوئي يعمل بواسطة المخرج العائم في الـ MOSFET كذلك يقدم دراسة جديدة لحالات الانبعاث الحراري أو الضوئي ويعطي إمكانية التغيرات المطلوبه عند الاستخدام ويضمن هذا المصدر التحكم في حالة التسرب التيارات في الحالات المسموح بها ومن أهمية هذا المصدر الكهروضوئي أيضاً سهولة تركيبه وتشكيله على أي دوائر الكترونية .

.....

20

.....

.....